Accepted manuscript of: H. Li and J. Zhang, "Towards Sustainable Integration: Techno-Economic Analysis and Future Perspectives of Co-Located Wind and Hydrogen Energy Systems," Journal of Mechanical Design, vol. 146, no. 2, 020903, 2024. Version of record (DOI 10.1115/1.4063971): https://doi.org/10.1115/1.4063971
Copyright © 2023 by ASME. Originally published by ASME (The American Society of Mechanical Engineers).

Towards Sustainable Integration: Techno-Economic Analysis and Future Perspectives of Co-located Wind and Hydrogen Energy Systems

Honglin Li[*]
The University of Texas at Dallas
Richardson, TX 75080
Email: honglin.li@utdallas.edu

Jie Zhang[†]
The University of Texas at Dallas
Richardson, TX 75080
Email: jiezhang@utdallas.edu

ABSTRACT

This paper presents a comprehensive study that focuses on the techno-economic analysis of co-located wind and hydrogen energy integration within an Integrated Energy System (IES). The research investigates four distinct cases, each exploring various configurations of wind farms, electrolyzers, batteries, hydrogen storage tanks, and fuel cells. To obtain optimal results, the study employs a sophisticated mathematical optimization model formulated as a mixed-integer linear program. This model helps determine the most suitable component sizes and hourly energy scheduling patterns. The research utilizes historical meteorological data and wholesale market prices from diverse regions as inputs, enhancing the study's applicability and relevance across different geographical locations. Moreover, sensitivity analyses are conducted to assess the impact of hydrogen prices, regional wind profiles, and potential future fluctuations in component prices. These analyses provide valuable insights into the robustness and flexibility of the proposed IES configurations under varying market conditions and uncertainties. The findings reveal cost-effective system configurations, strategic component selections, and implications of future energy scenarios. Specifically comparing to configurations that only have wind and battery combinations, we find that incorporating an electrolyzer results in a 7% reduction in the total cost of the IES, and utilizing hydrogen as the storage medium for fuel cells leads to a 26% cost reduction. Additionally, the IES with hybrid hydrogen and battery energy storage achieves even higher and stable power output. This research facilitates decision-making, risk mitigation, and optimized investment strategies, fostering sustainable planning for a resilient and environmentally friendly energy future.

Keywords: Wind energy, hydrogen, integrated energy system, techno-economic analysis, sustainability.

Nomenclature

$\mathcal{B}$ Storage systems
$\mathcal{H}$ Time steps
$\mathcal{T}$ Technologies
$\mathcal{T}^{\text{gh}} \subseteq \mathcal{T}$ Technologies that generate hydrogen
$\mathcal{T}^{\text{h}} \subseteq \mathcal{T}$ Technologies that burn hydrogen

---

[*]Ph.D. Student, Department of Mechanical Engineering and the Center for Wind Energy.
[†]Associate Professor, Department of Mechanical Engineering, Department of Electrical and Computer Engineering (Affiliated), and the Center for Wind Energy (Affiliated), ASME Professional Member. Address all correspondence to this author.

$\mathcal{T}_b \subseteq \mathcal{T}$ Technologies that can charge storage system b
c_t^{cm} Slope of capital cost curve for technology t [\$/kW]
c_t^{cb} y-intercept of capital cost curve for technology t [\$]
c_b^{kW} Capital cost of power capacity for storage system b [\$/kW]
c_b^{bkWh} Capital cost of energy capacity for storage system b [\$/kWh]
c_b^{omb} Operation and maintenance cost of storage system b per unit of energy rating [\$/kWh]
$c_t^{\mathrm{om\sigma}}$ Operation and maintenance cost of technology t per unit of power rating [\$/kW]
c_t^{omb} Operation and maintenance cost of technologies using hydrogen t per unit of energy rating [\$/kWh]
c^{ome} Operation and maintenance cost of electrolyzer per unit of energy rating [\$/kg]
c_h^{e} Export rate for energy in time step h [\$/kWh]
c_h^{hts} Export rate for hydrogen in time step h [\$/kg]
$\bar{\delta}_h^{\mathrm{g}}$ Grid interconnection limit [kW]
δ_h^{d} Grid power demand [kW]
i_t^{r} Incentive rate for technology t [\$/kWh]
$\bar{l}_t^{\sigma}$ Upper incentive limit for technology t [\$]
f^{tow} Tax rate factor for owner [fraction]
f^{om} Operation and maintenance present worth factor [unitless]
f^{e} Energy present worth factor [unitless]
f_t^{pi} Present worth factor for incentives for technology t [unitless]
f_t^{li} Levelization factor of production incentive for technology t [fraction]
f_{th}^{p} Production factor of technology t at time step h [unitless]
f_e^{l} Levelization factor of technology t [fraction]
f_{eh}^{p} Production factor of electrolyzer at time step h [unitless]
$\bar{b}_t^{\sigma}$ Maximum power rating for technology t [kW]
η_{bt}^{+} Efficiency of charging storage system b using technology t [fraction]
η_b^{-} Efficiency of discharging storage system b [fraction]
$\underline{w}_b^{\mathrm{bkWh}}$ Minimum energy capacity of storage system b [kWh]
$\bar{w}_b^{\mathrm{bkWh}}$ Maximum energy capacity of storage system b [kWh]
$\bar{w}_b^{\mathrm{bkW}}$ Maximum power output of storage system b [kW]
$\underline{w}_b^{\mathrm{bkW}}$ Minimum power output of storage system b [kW]
$\bar{w}_b^{\mathrm{mcp}}$ Maximum percent state of charge of storage system b [fraction]
w_b^0 Initial percent state of charge of storage system b [fraction]
m_f Slope of the hydrogen rate curve for fuel cells [kg/kW]
m_e Slope of the power curve for electrolyzer [kW/kg]
X_t^{σ} Power rating of technology t [kW]
X_b^{kWh} Energy rating for storage system b [kWh]
X_b^{kW} Power rating for storage system b [kW]
X_{th}^{rp} Rated production of technology t during time step h [kW]
X_{eh}^{rp} Rated production of electrolyzer during time step h [kg/h]
X_{bh}^{stg} Exports from storage b to the grid during time step h [kW]
X_{th}^{ptg} Exports from technology t to the grid during time step h [kW]
X_{eh}^{sell} Hydrogen sold during time step h [kg]
X_t^{pi} Production incentive collected for technology t [\$]
$X_{b,0}^{\mathrm{se}}$ State of charge of storage system b at the end of time step 0 [kWh]
X_{bh}^{se} State of charge of storage system b at the end of time step h [kWh]
X_{bth}^{pts} Power from technology t used to charge storage system b during time step h [kW]
X_{bh}^{dfs} Power discharged from storage system b during time step h [kW]
X_{th}^{pte} Power from technology t supplied to the electrolyzer during time step h [kW]
X_{th}^{ptc} Curtailed power from technology t during time step h [kW]
X_{bh}^{ste} Power from storage b supplied to the electrolyzer during time step h [kW]
X_{eh}^{rp} Rated production of electrolyzer during time step h [kg/h]
X_e^{kg} Capacity of electrolyzer [kg/h]
X_{th}^{sh} State of charge of hydrogen tank during time step h [kg]
X_{eh}^{etf} Hydrogen to fuel cells during time step h [kg]
X_{fh}^{rp} Rated production of fuel cells during time step h [kW]
X_{fh}^{ftg} Power to grid from fuel cells during time step h [kW]

X_f^{kW} Capacity of fuel cells [kW]
Z_{th}^{to} 1 if technology t is operating in time step h; 0 otherwise [unitless]
Z_t^{pi} 1 if production incentive is available for technology; 0 otherwise [unitless]
M Arbitrary large number [unitless]

1 Introduction

The global pursuit of sustainable and environmentally friendly energy sources has witnessed unprecedented momentum in recent years [1]. As concerns about climate change and the depletion of fossil fuel resources escalate, the urgency to transition towards renewable energy solutions has become paramount [2]. Among these renewable alternatives, wind energy has emerged as a pivotal player, harnessing the power of nature's winds to generate clean electricity [3]. Wind power has experienced rapid growth and remarkable advancements, contributing significantly to the global energy mix and reducing greenhouse gas emissions; investment in wind generation saw a remarkable 20% increase in 2022 [4]. However, despite its numerous benefits, wind energy's inherent variability poses challenges for grid integration and stability [5].

One of the key challenges faced by wind power is its intermittency – the natural fluctuations in wind speed and direction that lead to varying energy output. Unlike conventional fossil fuel power plants that can be adjusted to meet demand, wind turbines generate electricity solely based on wind availability, leading to mismatches between energy production and consumption. As a result, the intermittent nature of wind energy can strain grid operations, potentially leading to grid instability and the need for expensive backup power sources [6–8].

To address these challenges and unlock the full potential of wind energy, the concept of power smoothing has emerged as a promising solution [9,10]. Power smoothing involves the deployment of energy storage systems that can capture surplus energy during periods of high wind availability and release it during low wind periods, effectively balancing the power supply and demand [11–13]. This mitigates the intermittent nature of wind energy and enables a consistent and predictable supply to the grid.

A wide array of energy storage technologies exists, including batteries [14], flywheel systems [13], pumped hydro storage [15], and compressed air energy storage [16]. These conventional storage methods have been widely explored and have proven effective in supporting renewable energy integration. Prior research underscores the importance of efficient energy storage and power smoothing solutions for the successful grid integration of wind energy. However, while these methods have proven effective, they may present limitations concerning scalability, environmental impact, or cost-effectiveness [17].

In recent years, there has been a notable shift towards exploring innovative and sustainable energy storage solutions, with hydrogen energy emerging as as a highly promising and transformative candidate [1, 5, 6, 18]. Hydrogen's unique attributes as an energy carrier make it exceptionally well-suited for power smoothing and renewable energy integration. Notably, its ability to be stored over extended periods allows for seasonal storage and flexible deployment, precisely when energy demand dictates. Moreover, hydrogen can serve multiple purposes, ranging from electricity generation [19], transportation [20], industrial processes [21], to heat production [22]. This versatility positions hydrogen as a dynamic and transformative energy vector, with the potential to revolutionize various sectors of the economy. Hydrogen is the most abundant element in the universe and can be produced through various methods, including electrolysis [23–25], steam methane reforming [26], and biomass gasification [27]. Of particular note, power-to-hydrogen (P2H) technologies capitalize on excess electricity, such as surplus wind energy, to produce hydrogen through electrolysis, offering a promising pathway for large-scale energy storage.

1.1 Literature Review

Despite the promising aspects of hydrogen-based energy storage, there is a need for in-depth techno-economic analysis to provide a comprehensive understanding of its practical applicability, especially in the context of wind power smoothing. The field of techno-economic analysis of hydrogen energy for wind energy power smoothing has garnered significant attention over the past few years. Researchers and experts have explored various aspects of integrating hydrogen technology into wind energy systems to address the intermittency and variability challenges associated with renewable energy sources. Here we provide a concise overview of the current state of the art in integrated wind and hydrogen systems, which can be categorized into four main areas.

Hydrogen Production Technologies for Wind Energy Integration: The pursuit for efficient and sustainable energy solutions has spurred numerous studies exploring various hydrogen production methods that can seamlessly complement and enhance wind energy systems. Among the prominent contenders, electrolysis, in particular, has emerged as a promising candidate, offering innovative avenues for harnessing excess wind energy and converting it into valuable hydrogen resources. Two primary forms of electrolysis have taken the spotlight: proton exchange membrane electrolysis [28] and alkaline electrolysis [29]. Both methods have been subjected to thorough examination, highlighting their remarkable capabilities in facilitating the conversion of surplus wind power into clean, storable hydrogen fuel. Apart from electrolysis, researchers have also delved into alternative avenues to achieve optimal hydrogen production alongside wind energy integration. One

such approach entails methane reforming [30], which has captivated attention for its potential to effectively harness wind energy and convert methane into hydrogen, thereby presenting a compelling pathway for energy conversion and storage.

Hydrogen Storage and Transportation: The efficient storage and seamless transportation of hydrogen constitute pivotal pillars in the pursuit of transforming it into a highly viable and effective option for power smoothing within the realm of wind energy. Over the years, extensive research has diligently explored and evaluated a diverse range of hydrogen storage techniques, each holding the potential to unlock the full promise of this clean, abundant fuel source. One of the primary avenues investigated is compressed hydrogen storage [31], wherein hydrogen gas is compressed at high pressures and stored in specially designed containers. This approach offers an impressive balance between energy density and practicality, making it suitable for a variety of applications, including wind energy power smoothing. The advancement in materials and engineering techniques has significantly enhanced the safety and efficacy of compressed hydrogen storage solutions, further solidifying its appeal. Another avenue of investigation lies in the domain of liquid hydrogen storage [32], wherein hydrogen is cooled and maintained at cryogenic temperatures to exist in a liquid state. This method capitalizes on the superior energy density of liquid hydrogen, allowing for increased storage capacity and extended usability. While presenting unique challenges due to the need for cryogenic systems, liquid hydrogen storage has shown great potential, especially in long-term energy storage scenarios where maximizing capacity is essential. In tandem with storage advancements, researchers have diligently explored various transportation methods, aiming to efficiently move hydrogen from production sites to end-users or dedicated energy storage facilities. Among these methods, pipelines [33] stand out as a primary choice for large-scale transportation, offering a cost-effective and reliable means of conveying hydrogen over significant distances. Investment in pipeline infrastructure for hydrogen has been growing, with the potential to form extensive networks that connect diverse regions and enable widespread adoption of hydrogen energy.

Hydrogen Integration Strategies in Wind Farms: The pursuit of maximizing the potential of renewable energy sources has sparked considerable interest in integrating hydrogen technologies within wind farms. This innovative approach aims to revolutionize power generation and elevate system flexibility to new heights. A plethora of studies have delved into various configurations, each offering unique benefits and opportunities to establish a seamless synergy between wind energy and hydrogen production. One promising avenue of exploration involves establishing co-located hydrogen production facilities within wind farms [34]. By situating hydrogen production units in close proximity to wind turbines, surplus energy can be efficiently harnessed during periods of high wind generation. The excess electricity can then be diverted into the hydrogen production process, enabling the transformation of water into hydrogen through electrolysis. This integration not only provides a valuable means of energy storage but also unlocks the potential to utilize hydrogen as a clean, eco-friendly fuel for various applications, further enhancing the overall sustainability of the system. Furthermore, researchers have explored centralized hydrogen storage systems to complement wind farms [35]. In this configuration, excess energy from multiple wind turbines is channeled into a centralized hydrogen storage facility. This approach facilitates optimal use of the surplus electricity, ensuring that wind power does not go to waste during periods of low demand. The stored hydrogen can then be utilized for various applications, ranging from power generation during peak demand hours to supplying clean fuel for vehicles or industrial processes, thereby adding a layer of versatility to the integrated system.

Techno-Economic Analysis and Optimization Models: To gauge the feasibility and potential benefits of integrating hydrogen energy with wind power, researchers have devised sophisticated techno-economic models and optimization frameworks [36–40]. These analytical tools serve as crucial instruments in evaluating the economic viability and sustainability of such integrated systems. By considering a myriad of factors, these models provide comprehensive insights into the most optimal and cost-effective pathways for successfully implementing hydrogen integration within wind energy systems. A key aspect analyzed by these models is the capital and operational costs associated with various components of the integrated system. This includes costs related to installing hydrogen production facilities, storage infrastructure, and hydrogen utilization technologies. The models carefully weigh these expenditures against potential savings and revenue streams generated from hydrogen sales or usage, ultimately determining the financial viability of the integrated setup. Furthermore, energy efficiency is a critical parameter taken into account by these models. The efficiency of hydrogen production methods, storage systems, and utilization technologies significantly impacts the overall performance and viability of the integrated system. Researchers meticulously assess different technology options to ensure that the overall energy conversion and utilization process is as efficient as possible, minimizing losses and maximizing the system's overall efficiency.

1.2 Research Contributions

This paper presents a holistic and innovative approach to optimize renewable energy integration by leveraging hydrogen-based energy storage for enhanced wind farm stability. Through a rigorous exploration of various system configurations, addressing existing gaps in the literature, and considering the influence of regional meteorological conditions and future equipment costs, this study contributes valuable insights that advance the seamless integration of renewable energy sources into the power grid. The key contributions of this research can be summarized as follows:

1. **Comprehensive System Integration with Hydrogen-based Storage:** By considering a wide range of system configurations, the research provides holistic insights into how hydrogen storage complements and enhances the stability and

reliability of wind farms.

2. **Utilization of Excess Wind Energy for Hydrogen Production:** By converting surplus wind power into hydrogen through electrolysis, the study showcases a sustainable approach to energy storage, thus maximizing the utilization of curtailed wind energy.
3. **Evaluation of Hydrogen Storage and Fuel Cells for Energy Conversion:** This study evaluates the effective of both hydrogen storage and fuel cell technologies for efficient energy conversion.
4. **Sensitivity Analysis on Future Equipment Costs:** Recognizing the dynamic nature of the energy landscape, the study conducts sensitivity analyses on future equipment costs.
5. **Regional Meteorological Impacts on Wind Farm Stability:** Taking into account the influence of regional meteorological conditions, the research sheds light on how climate variations can affect wind farm stability and performance.

The paper's remaining content is structured as follows: Section 2 outlines the techno-economic methodology applied in this study. Section 3 illustrates the case studies and their corresponding results, considering various combinations of Integrated Energy System (IES) components. Finally, Section 4 summarizes the findings, draws conclusions, and delves into potential areas for future research.

2 Techno-Economic Analysis Methodology

The techno-economic analysis for the sector-coupled wind-hydrogen IES is performed using the open-source techno-economic tool, REopt (Renewable Energy Integration and Optimization), developed by the National Renewable Energy Laboratory (NREL) [41]. Fig. 1 depicts the overall framework of the REopt analysis for the integrated wind and hydrogen system. REopt takes into account various factors, including weather conditions, electrical load, wholesale electricity prices, and hydrogen prices at the system's location, to determine the capacity and dispatch decisions for the components of the IES. The primary objective is to optimize economic savings or profits from on-site energy production while maximizing stabilized power output. It should be noted that REopt is best suited for site-specific studies and is implemented through net export or import limits to the system, rather than for system-level analyses.

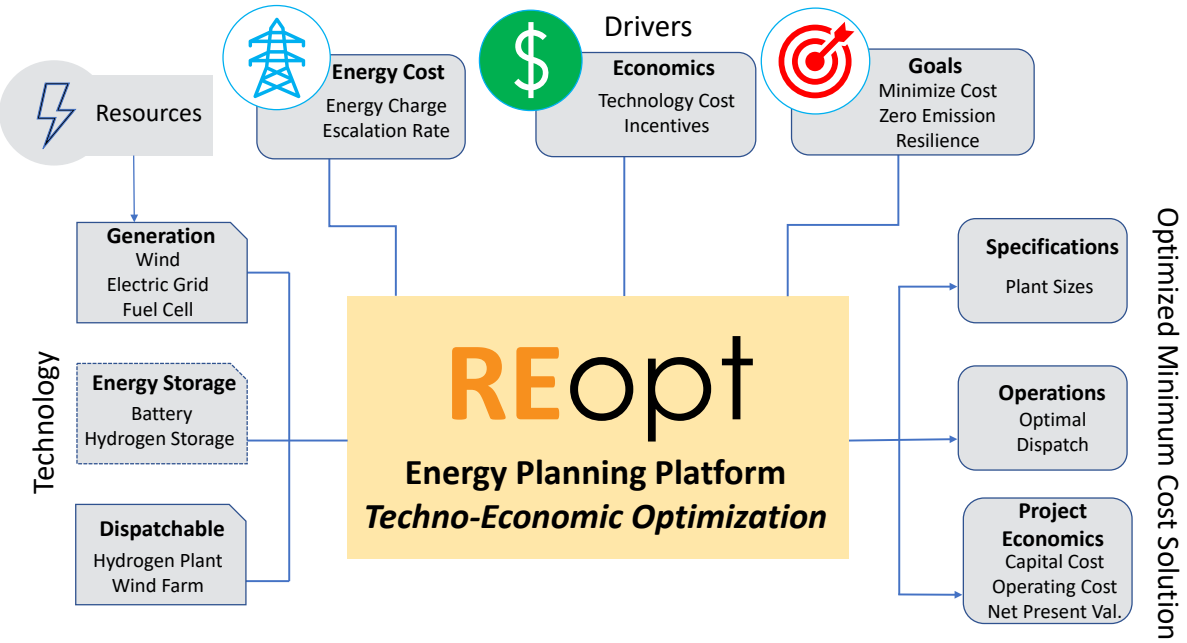


Fig. 1: Techno-economic analysis framework for the integrated wind and hydrogen system (modified from [36])

In our study, we have extended the capabilities of REopt by incorporating additional models for the electrolyzer, hydrogen tank storage, and hydrogen fuel cell. Fig. 2 illustrates the overall architecture of the REopt modules used in this study, along with the input and output parameters of each component and their respective constraints. To model the IES, certain user-inputs are provided to REopt, including the capital cost, operations and maintenance (O&M) cost, annual electricity consumption, battery charging and discharging efficiency, and other relevant performance parameters of the wind energy

system. These inputs enable the estimation of power generation for the wind and battery components. For the hydrogen production model, the electrolyzer technology is employed, which utilizes electricity and a feedstock like water to produce hydrogen. User-inputs for the electrolyzer in REopt include the capital and O&M costs, feedstock type, electric energy consumed to hydrogen produced ratio, hydrogen sale price, and other relevant parameters [4, 42–44]. The hydrogen storage tank is modeled with considerations for minimum and maximum capacity limits, installation cost, and O&M cost [43, 45]. These inputs help determine the appropriate storage capacity for the hydrogen system. Various financial parameters, such as tax rates, investment-based incentives, capital-based incentives, production-based incentives, discount rate, and modified accelerated cost recovery system (MACRS), are also taken into account. These financial inputs are crucial for obtaining realistic results that consider the economic aspects of the integrated wind-hydrogen system.



Fig. 2: Model architecture of the REopt modules adopted/created in this study (modified from [36])

By incorporating the electrolyzer, hydrogen tank, and fuel cell technology into the existing REopt capability, we can now assess the techno-economic performance of wind and hydrogen IES under various conditions, including different meteorological conditions, fluctuating electricity and hydrogen prices, and more. Fig. 3 depicts the overall structure of the grid-connected IES with wind, battery, hydrogen, and fuel cells in this study. We have comprehensively explored and compared the following four scenarios.

1. **Case I: Wind+Battery (Base Scenario)**: This case involves a wind power plant integrated with a conventional energy storage device. The objective is to minimize system costs while achieving maximum stabilized output power. It is assumed in this study that the maximum stabilized output power of the system aligns with the grid demand. This approximation is derived from extensive empirical analyses. Thus, it's important to note that, within the scope of this study, we do not account for any potential grid demand deficits. The mathematical model optimizes the capacity and power size of the energy storage device, ensuring efficient utilization of wind energy and enhancing grid stability.
2. **Case II: Wind+Battery+Electrolyzer (Electrolyzer Integration)**: In this case, an electrolyzer is added to the system to convert excess wind energy into hydrogen, thereby increasing system revenue and energy versatility. The optimization process determines the optimal sizes of the electrolyzer and energy storage device to maximize hydrogen generation and storage while minimizing costs.
3. **Case III: Wind+Electrolyzer+Hydrogen Tank+Fuel Cell (Hydrogen Storage and Fuel Cell Integration)**: This case replaces conventional battery energy storage with hydrogen storage and a fuel cell. The economic feasibility of this combination is assessed, considering the lack of battery state-of-charge (SOC) limitations, ensuring optimal energy storage and utilization. The integration of hydrogen storage and fuel cells enhances energy conversion efficiency and offers a cleaner and sustainable energy option.
4. **Case IV: Wind+Battery+Electrolyzer+Hydrogen Tank+Fuel Cell (Comprehensive Integration)**: This case represents a holistic approach, incorporating electrolyzers, hydrogen tanks, fuel cells, and traditional battery storage. A sensitivity analysis examines the impact of future equipment cost reduction on system costs, providing valuable insights for long-term planning and investment strategies. Additionally, grid power integration is explored to enhance wind farm stability during low wind periods and maximize curtailed wind energy utilization. This comprehensive integration optimizes the synergies between different components, offering an efficient and resilient renewable energy system.

The modeling of the IES is a complex process that involves considering multiple technology, system, and financial constraints. These constraints encompass energy balance, battery and storage tank states, technology capacities, grid import/export limits, and stabilized output requirements. The primary objective of the optimization is to minimize the total cost of the IES, which includes installation costs for the electrolyzer, wind energy system, batteries, hydrogen storage, and fuel cells (if applicable), as well as O&M costs, electricity purchases, taxes, incentives, and profits from electricity and hydrogen sales. The objective function is formulated as:

$$
\begin{aligned}
\text{Minimize} \quad & \underbrace{\sum_{t\in\mathcal{T}}\left(c_t^{\text{cm}}\cdot X_t^{\sigma}+c_t^{\text{cb}}\cdot Z_t^{\sigma}\right)}_{\text{Generating Technology Capital Costs}} + \underbrace{\sum_{b\in\mathcal{B}}\left(c_b^{\text{kW}}\cdot X_b^{\text{bkW}}+\left(c_b^{\text{kWh}}+c_b^{\text{omb}}\right)\cdot X_b^{\text{bkWh}}\right)}_{\text{Storage Capital Costs}} + \\
& (1-f^{\text{tow}})\cdot f^{\text{om}}\cdot\left(\underbrace{\sum_{t\in\mathcal{T}}c_t^{\text{om}\sigma}\cdot X_t^{\sigma}}_{\text{Fixed O\&M Costs}}+\underbrace{\sum_{t\in\mathcal{T}^{\text{h}},h\in\mathcal{H}}c_t^{\text{omp}}\cdot X_{th}^{\text{rp}}}_{\text{Variable O\&M Costs}}+\underbrace{c^{ome}\cdot X_{eh}^{\text{rp}}}_{\text{Electrolyzer O\&M costs}}\right)- \\
& (1-f^{\text{tow}})\cdot f^{e}\cdot\left(\underbrace{\sum_{h\in\mathcal{H}}\left(c_h^{\text{e}}\cdot X_h^{\text{stg}}+\sum_{t\in\mathcal{T}}c_h^{\text{e}}\cdot X_{th}^{\text{ptg}}\right)}_{\text{Energy Export Payment}}+\underbrace{\sum_{h\in\mathcal{H}}c_h^{\text{hts}}\cdot X_{eh}^{\text{sell}}}_{\text{Hydrogen profit}}\right)-(1-f^{\text{tow}})\cdot\underbrace{\sum_{t\in\mathcal{T}}X_t^{\text{pi}}}_{\text{Production Incentives}}
\end{aligned}
\tag{1}
$$

The following constraints are considered in the optimization.

$$
X_{th}^{\text{rp}} \leq \underbrace{\bar{b}_t^{\sigma}\cdot Z_{th}^{\text{to}}}_{\text{Maximum Power Rating}} \qquad \forall t\in\mathcal{T}, h\in\mathcal{H} \tag{2}
$$

Constraint (2) ensures that the system's output is restricted to its maximum power rating when it is turned on, and it must be 0 when it is off.

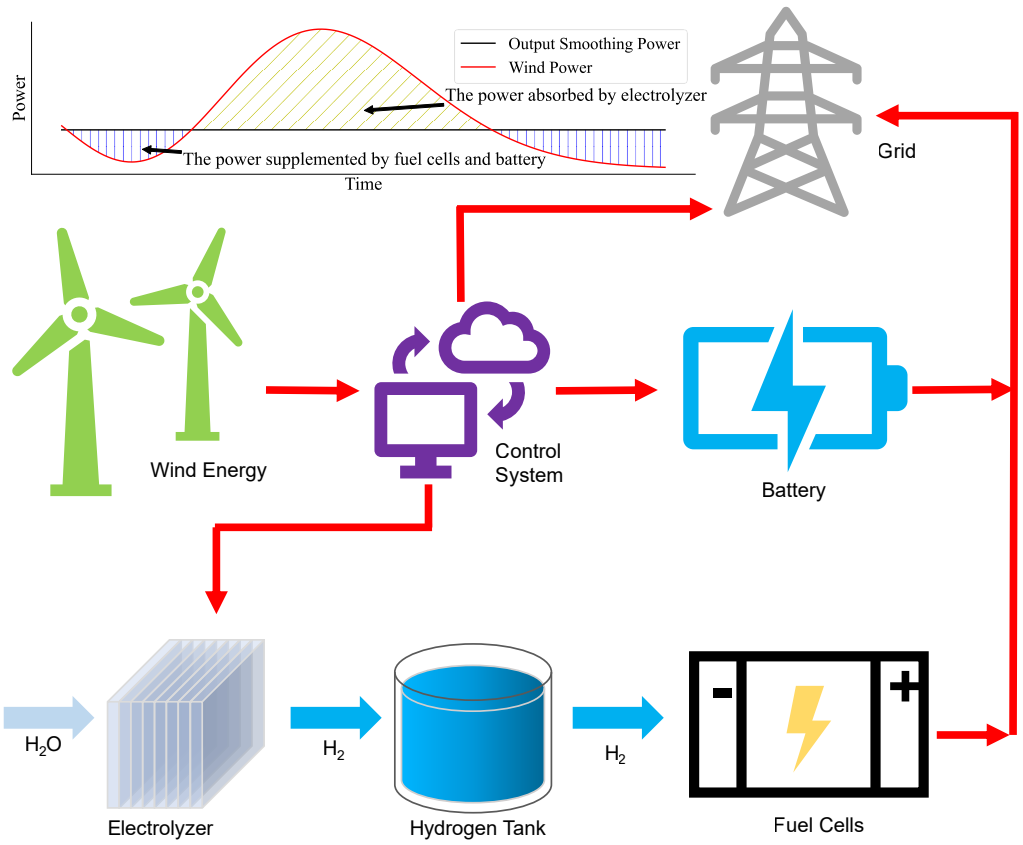


Fig. 3: Overall structure of the grid-connected IES with wind, battery, hydrogen, and fuel cells

$$X_{b,0}^{\mathrm{se}} = \underbrace{w_b^0 \cdot X_b^{\mathrm{bkWh}}}_{\text{Initial State of Charge}} \qquad \forall b \in \mathcal{B} \tag{3}$$

$$\underline{w}_b^{\mathrm{bkWh}} \leq X_b^{\mathrm{bkWh}} \leq \bar{w}_b^{\mathrm{bkWh}} \quad \forall b \in \mathcal{B} \tag{4}$$

$$\underline{w}_b^{\mathrm{bkW}} \leq X_b^{\mathrm{bkW}} \leq \bar{w}_b^{\mathrm{bkW}} \quad \forall b \in \mathcal{B} \tag{5}$$

Constraint (3) establishes the initial state of charge for each storage system as a fraction of its total energy rating. Constraints (4) and (5) further constrain the size of the storage system by imposing lower and upper bounds on its energy capacity and power output, respectively. These bounds limit the range within which the energy capacity and power output of the storage system can be optimized.

$$X_{bh}^{\mathrm{se}} = X_{b,h-1}^{\mathrm{se}} + \underbrace{\sum_{t \in \mathcal{T}} \left(\eta_{bt}^{+} \cdot X_{bth}^{\mathrm{pts}} \right) - X_{bh}^{\mathrm{dfs}} / \eta_b^{-}}_{\text{Net Charging Energy}} \quad \forall b \in \mathcal{B}, h \in \mathcal{H} \tag{6}$$

$$X_{bh}^{\mathrm{se}} \geq \underbrace{\underline{w}_b^{\mathrm{mcp}} \cdot X_b^{\mathrm{bkWh}}}_{\text{Minimum State of Charge}} \qquad \forall b \in \mathcal{B}, h \in \mathcal{H} \tag{7}$$

Constraint (6) ensures inventory balance for the state of charge of storage system b at the end of time period h. Constraint (7) enforces a minimum state of charge requirement for the energy stored in the battery. This constraint ensures that the energy in the battery does not fall below the specified minimum level.

$$X_b^{\mathrm{kW}} \geq \underbrace{\sum_{t \in \mathcal{T}_b} X_{bth}^{\mathrm{pts}} + X_{bh}^{\mathrm{dfs}}}_{\text{Charging and Discharging Power}} \qquad \forall b \in \mathcal{B}, h \in \mathcal{H} \tag{8}$$

$$X_b^{\mathrm{bkWh}} \geq X_{bh}^{\mathrm{se}} \quad \forall b \in \mathcal{B}, h \in \mathcal{H} \tag{9}$$

Constraint (8) restricts the power that can be charged or discharged from the storage system in each time step to the storage system's power rating. Additionally, constraint (9) sets a limit on the amount of energy stored in the storage system in each time step to the storage system's energy capacity.

$$X_t^{\mathrm{pi}} \leq \min \left\{ M \cdot Z_t^{\mathrm{pi}}, \underbrace{\sum_{h \in \mathcal{H}} i_t^{\mathrm{r}} \cdot f_t^{\mathrm{pi}} \cdot f_{th}^{\mathrm{p}} \cdot f_t^{\mathrm{li}} \cdot X_{th}^{\mathrm{rp}}}_{\text{Total Production Incentives}} \right\} \quad \forall t \in \mathcal{T} \tag{10}$$

$$X_t^{\sigma} \leq \underbrace{\bar{i}_t^{\sigma} + \bar{b}_t^{\sigma} \cdot \left(1 - Z_t^{\mathrm{pi}}\right)}_{\text{Upper Bound on the System Size}} \qquad \forall t \in \mathcal{T} \tag{11}$$

Constraint (10) computes the total production incentives, if they are available, for each technology. Constraint (11) sets an upper bound on the system size that qualifies for production incentives.

$$\underbrace{f_{eh}^{\mathrm{p}} \cdot f_e^{\mathrm{l}} \cdot X_{eh}^{\mathrm{rp}}}_{\text{Actual Power of Electrolyzer}} = X_{eh}^{\mathrm{p}} \quad \forall h \in \mathcal{H} \tag{12}$$

$$m_e \cdot X_{eh}^{\mathrm{p}} = \underbrace{\sum_{t \in \mathcal{T}} X_{th}^{\mathrm{pte}} + \sum_{b \in \mathcal{B}} X_{bh}^{\mathrm{ste}}}_{\text{Total Energy Input to the Electrolyzer}} \qquad \forall h \in \mathcal{H} \tag{13}$$

$$X_{eh}^{\mathrm{rp}} \leq X_e^{\mathrm{kg}} \quad \forall h \in \mathcal{H} \tag{14}$$

Constraints (12) and (13) give the input-output relationship and energy balance equations for the electrolyzer operation process, respectively. Constraint (14) sets a limit on the production of the eletrolyzer to the electrolyzer capacity.

$$X_{th}^{\mathrm{sh}} = X_{t,h-1}^{\mathrm{sh}} + \underbrace{X_{eh}^{\mathrm{p}} - X_{eh}^{\mathrm{sell}} - X_{eh}^{\mathrm{etf}}}_{\text{Net Hydrogen Storage}} \quad \forall h \in \mathcal{H} \tag{15}$$

$$X_{th}^{\mathrm{sh}} \leq X^{\mathrm{tank}} \quad \forall h \in \mathcal{H} \tag{16}$$

Constraint (15) ensures inventory balance for the state of charge of hydrogen storage system at the end of time period h. Constraint (16) sets a limit on the amount of hydrogen stored in the hydrogen storage system in each time step to the hydrogen storage system's capacity.

$$\underbrace{f_{fh}^{\mathrm{p}} \cdot f_{f}^{1} \cdot X_{fh}^{\mathrm{rp}} \cdot m_{f}}_{\text{Actual Hydrogen Consumption in Fuel Cells}} = X_{eh}^{\mathrm{etf}} \quad \forall f \in \mathcal{T}^{h}, h \in \mathcal{H} \tag{17}$$

$$\underbrace{f_{fh}^{\mathrm{p}} \cdot f_{f}^{1} \cdot X_{fh}^{\mathrm{rp}}}_{\text{Actual Energy Generation from Fuel Cells}} = X_{fh}^{\mathrm{ftg}} \quad \forall f \in \mathcal{T}^{h}, h \in \mathcal{H} \tag{18}$$

$$X_{fh}^{\mathrm{rp}} \leq X_{f}^{\mathrm{kW}} \quad \forall h \in \mathcal{H} \tag{19}$$

Constraints (17) and (18) give the relationship between the demand for hydrogen and the production of electricity and its capacity at each time point of the hydrogen fuel cells, respectively. Constraint (19) sets a limit that hydrogen fuel cells cannot generate more power per hour than their capacity.

$$\underbrace{\sum_{t \in \mathcal{T}} f_{th}^{\mathrm{p}} \cdot f_{t}^{1} \cdot X_{th}^{\mathrm{rp}}}_{\text{Actual Wind Energy Generation}} + \sum_{b \in \mathcal{B}} X_{bh}^{\mathrm{dfs}} = \underbrace{\sum_{t \in \mathcal{T}} \left(\sum_{b \in \mathcal{B}} X_{bth}^{\mathrm{pts}} + X_{th}^{\mathrm{ptg}} + X_{th}^{\mathrm{pte}} + X_{th}^{\mathrm{ptc}} \right)}_{\text{Total Wind Energy Generation}} + \underbrace{\sum_{b \in \mathcal{B}} \left(X_{bh}^{\mathrm{ste}} + X_{bh}^{\mathrm{stg}} \right)}_{\text{Total Battery Discharge}} \quad \forall h \in \mathcal{H} \tag{20}$$

$$\underbrace{\sum_{t \in \mathcal{T}} X_{th}^{\mathrm{ptg}} + \sum_{b \in \mathcal{B}} X_{bh}^{\mathrm{stg}}}_{\text{Energy Delivered to the Grid}} = \delta_{\mathrm{h}}^{\mathrm{d}} \quad \forall h \in \mathcal{H} \tag{21}$$

$$\sum_{t \in \mathcal{T}} f_{th}^{\mathrm{p}} \cdot f_{t}^{1} \cdot X_{th}^{\mathrm{rp}} = \sum_{t \in \mathcal{T}} \left(\sum_{b \in \mathcal{B}} X_{bth}^{\mathrm{pts}} + X_{th}^{\mathrm{ptg}} + X_{th}^{\mathrm{pte}} + X_{th}^{\mathrm{ptc}} \right) \quad \forall h \in \mathcal{H} \tag{22}$$

$$\sum_{b \in \mathcal{B}} X_{bh}^{\mathrm{stg}} + \sum_{t \in \mathcal{T}} X_{th}^{\mathrm{ptg}} \leq \bar{\delta}_{\mathrm{h}}^{\mathrm{g}} \quad \forall h \in \mathcal{H} \tag{23}$$

Constraint (20) ensures that the load is balanced by equating the sum of power from all generation technologies and energy storage systems. Constraint (21) allows both storage X_{h}^{stg} and production X_{h}^{ptg} to contribute to the energy delivered to the grid, but the total contribution must equal the power demand, which is also the stabilized output power of the system. Constraint (22) limits the power allocation to all generation technologies at each point in time. Constraint (23) ensures the transmitted power to the grid does not exceed the interconnection limit.

$$X_{b}^{\mathrm{kWh}}, X_{b}^{\mathrm{kW}} \geq 0 \quad \forall b \in \mathcal{B} \tag{24}$$

$$X_h^{\mathrm{stg}}, X_h^{\mathrm{ptg}} \geq 0 \quad \forall h \in \mathcal{H} \tag{25}$$

$$X_t^{\mathrm{pi}}, X_t^{\sigma} \geq 0 \quad \forall t \in \mathcal{T} \tag{26}$$

$$X_{bth}^{\mathrm{pts}} \geq 0 \quad \forall b \in \mathcal{B}, t \in \mathcal{T}, h \in \mathcal{H} \tag{27}$$

$$X_{th}^{\mathrm{pte}}, X_{th}^{\mathrm{ptc}}, X_{th}^{\mathrm{sh}}, X_{th}^{\mathrm{rp}} \geq 0 \quad \forall t \in \mathcal{T}, h \in \mathcal{H} \tag{28}$$

$$X_{bh}^{\mathrm{ste}}, X_{bh}^{\mathrm{dfs}}, X_{bh}^{\mathrm{se}}, X_{b,0}^{\mathrm{se}} \geq 0 \quad \forall b \in \mathcal{B}, h \in \mathcal{H} \tag{29}$$

$$X_{eh}^{\mathrm{rp}}, X_{eh}^{\mathrm{etf}}, X_{eh}^{\mathrm{p}}, X_{eh}^{\mathrm{sell}}, X_{eh}^{\mathrm{rp}} \geq 0 \quad \forall e \in \mathcal{T}^{gh}, h \in \mathcal{H} \tag{30}$$

$$X_e^{\mathrm{kg}} \geq 0 \quad \forall e \in \mathcal{T}^{gh} \tag{31}$$

$$X_{fh}^{\mathrm{rp}}, X_{fh}^{\mathrm{ftg}} \geq 0 \quad \forall f \in \mathcal{T}^{h}, h \in \mathcal{H} \tag{32}$$

$$X_f^{\mathrm{kW}} \geq 0 \quad \forall f \in \mathcal{T}^{h} \tag{33}$$

$$Z_{th}^{\mathrm{to}} \in \{0,1\} \quad \forall t \in \mathcal{T}, h \in \mathcal{H} \tag{34}$$

$$Z_t^{\mathrm{pi}} \in \{0,1\} \quad \forall t \in \mathcal{T} \tag{35}$$

Finally, constraints (24-33) ensure all of the variables in our formulation assume non-negative values. In addition to non-negativity restrictions, constraints (34, 35) establish the integrality of the appropriate variables.

REopt extends its functionality to provide comprehensive runtime support for the IES optimization model. This encompasses tasks such as modeling and simulating the various constituent modules within IES. Additionally, REopt plays a pivotal role in supplying coefficients to the optimization model, coordinating the entire optimization procedure, as well as efficiently handling the processing and dissemination of the resultant outcomes [41]. The problem is formulated as a mixed-integer linear program (MILP), and the FICO Xpress solver is utilized to find the optimal selection, sizing, and dispatch strategy of technologies from a candidate pool. Since the solver uses an exact algorithm rather than a heuristic algorithm to obtain the optimal solution, this optimal solution is also the global optimal solution. This approach ensures the maximization of stabilized power output at each time step while minimizing the overall life cycle cost of the system, encompassing both system costs and profit. The optimization process yields several important outputs, including the maximized stabilized output power, optimal component sizes, total system expenditure, capital expenditure for each component, the trade-off between wind and hydrogen production, the levelized cost of hydrogen (LCOH), and the levelized cost of energy (LCOE) of the IES. Additionally, various financial parameters such as payback period, life cycle cost, and net present value are provided, offering valuable insights for IES investment, planning, and operation decisions. This comprehensive modeling approach

empowers stakeholders with critical information for designing, optimizing, and managing the IES effectively, supporting the development of sustainable and economically viable energy solutions.

In this research, a single-year optimization approach is employed to estimate cash flows over an extended 25-year period, assuming constant production and consumption throughout the entire analysis period. This approach assumes perfect foresight in predicting all future events, encompassing factors like weather conditions and energy demand. While this method provides valuable insights, it is subject to several inherent limitations that can influence the results and their real-world applicability. These limitations stem from various assumptions made in the analysis, including the presumption of consistent wind energy generation, fixed electrolyzer efficiency, stable hydrogen storage costs, and simplified grid integration. Additionally, these analyses often rely on historical or estimated data, potentially introducing uncertainties into the findings. Furthermore, they may not fully account for the influence of technological advancements, environmental impacts, changing policies, or economic factors.

Key limitations of these studies include the omission of environmental costs and the oversight of potential technology breakthroughs. Regulatory changes, such as alterations in government policies or incentives, can significantly affect project economics, but these analyses often overlook such dynamics. Moreover, it's important to acknowledge that these studies are typically location-specific and may not readily generalize well to different regions with varying resource availability, infrastructure, and market conditions.

3 Numerical Experiments

In this study, the IES is assumed to be located in Snyder, TX, with a planned wind farm capacity of 253 MW, thus, the decision variable of wind farm size in this model will be fixed at 253 MW. Historical meteorological data from the year 2020, along with wholesale market prices from the Electric Reliability Council of Texas (ERCOT), serve as inputs for the study. Fig. 4 visually represents the annual wind power generation obtained from the simulation. The essential assumptions for setting up the hybrid energy system are summarized in Table 1, with a planning horizon of 25 years. To conduct the techno-economic analysis, the analysis employs 8,760 hourly data points for the modeled year (2020).

To enhance the conciseness of this paper while maintaining its focus, we have carefully selected key parameters for inclusion in Table 1. Our criteria for choosing these parameters are as follows:

Relevance to Key Components: We have included parameters that are essential for understanding the key components of our study.
Impact on Key Results: Parameters that significantly influence critical outcomes, such as LCOE and total cost, have been prioritized.
Focus on New Modules: In particular, we have focused on parameters related to the newly added module, the hydrogen system. For original modules like the wind system, we have relied on default parameters as described in [41].

For future projections, the study takes into account changes in grid energy costs and O&M expenses with a constant rate of change. This approach incorporates discounting factors to account for anticipated cost escalation or de-escalation rates. The study assumes perfect predictions of all future events, encompassing weather conditions and failure rates. Moreover, all costs and benefits are discounted using a specified discount rate to present values, following standard economic practices.

Capital and operating costs for wind, battery storage, various hydrogen generation technologies, fuel cell, and other system components are referenced from the NREL Annual Technology Baseline (ATB) [46]. This comprehensive approach allows for a robust analysis of the IES, enabling strategic decision-making and evaluation of economic viability and long-term sustainability over the planning period.

3.1 Results and Discussion

Table 2 presents a comprehensive overview of the optimal sizing of various components within the IES, including wind, electrolyzer, battery, tank, and hydrogen fuel cell, along with the corresponding total system costs for all four cases. The results indicate significant cost reductions in Case II (Electrolyzer Integration) and Case III (Hydrogen Storage and Fuel Cell Integration) by 7% and 26%, respectively, compared to the benchmark Case I. Particularly in Case III, battery storage is excluded and replaced by the integration of a hydrogen storage tank and fuel cell system.

In Case IV (Comprehensive Integration), the higher total system cost is attributed to the increased stabilized IES power output (i.e., 57 MW). In order to further evaluate the economic advantages of the Case IV combination, we added two additional sub-cases, which have the same stabilized IES output power as Case II and Case III, respectively, namely Case IV(a) and Case IV(b). When comparing the stabilized IES power outputs of 28.3 MW (Case IV(a)) and 39 MW (Case IV(b)) to Cases II and III, respectively, the total system cost in Case IV can be reduced by 23% and 26%. Notably, the curtailed rate of wind energy is lower in Case IV, suggesting the more efficient utilization of the electrolyzer, which was deliberately chosen to be smaller to meet the objective of minimizing the total system cost while maintaining maximum stabilized output. Indeed, Case III exhibits the lowest curtailed rate among all the cases due to its installation of the largest electrolyzer and

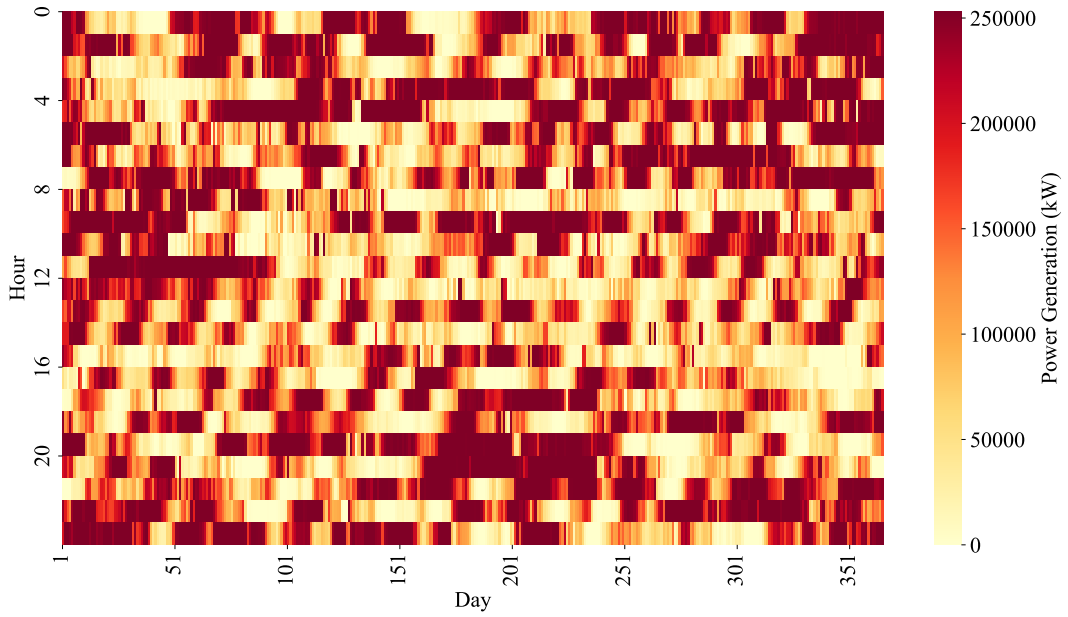


Fig. 4: The annual wind power generation of the simulated wind farm in 2020

Table 1: Key assumptions in the integrated energy system setup [4, 42–45]

Parameter	Cost
Electricity consumed per kg of hydrogen produced (low thermal energy)	55 kWh/kg
Hydrogen sale price	$2/kg
Hydrogen slope for fuel cell	0.076 kg/kWh
Electrolyzer installation cost	$48,000/kg/yr
Fixed electrolyzer O&M cost	$3,600/kg/yr
Variable electrolyzer O&M cost	$0.24/kg
Fuel cell installation cost	$500/kW
Fuel cell fixed O&M cost	$30/kW
Planning period	25 years
Minimum allowable battery SOC	0.2

its concerted effort to maximize the utilization of wind energy. However, it is essential to note that this configuration may not be the most economical option, as the utilization of the electrolyzer is not optimized sufficiently. This observation is further validated by the LCOH results, which indicate that Case III has the highest LCOH among all cases. Therefore, while the wind curtailed rate in Case III appears favorable, it must be cautiously interpreted in light of the higher LCOH and potential inefficiencies in the utilization of the electrolyzer. This information is crucial for the IES planning, as it highlights the trade-offs between curtailed rates and overall system economics and efficiency in the decision-making process.

These findings shed light on the cost-effective configurations and strategic component selections within the IES to achieve optimal performance and address energy demands efficiently. The outcomes provide valuable insights for decision-makers seeking to strike a balance between system costs, renewable energy utilization, and curtailment rates, while striving for a sustainable and economically viable integrated energy solution.

Fig. 5 provides a detailed view of the monthly energy output distribution for each component in the four cases. A comparison between Case I and Case II reveals that the addition of the electrolyzer in Case II, a power consumer component, results in a portion of the wind power being allocated to supply the electrolyzer. Despite the unchanged battery capacity

Table 2: Integrated energy system component capacity and cost

Technology	Case I	Case II	Case III	Case IV	Case IV (a)	Case IV (b)
Wind	253 MW	253 MW	253 MW	253 MW	253 MW	253 MW
Stabilized IES power	28.3 MW	28.3 MW	39 MW	57 MW	28.3 MW	39 MW
LCOE of wind	$0.0479/kWh	$0.0479/kWh	$0.0479/kWh	$0.0479/kWh	$0.0479/kWh	$0.0479/kWh
Fuel cell	N/A	N/A	39,000 kW	32,284 kW	25, 823 kW	33,001 kW
Hydrogen tank	N/A	N/A	185,236 kg	208,565 kg	59, 247 kg	128,573 kg
Battery energy capcity	1,064,030 kWh	1,064,030 kWh	N/A	867,950 kWh	54, 217 kWh	160,555 kWh
Battery power capcity	224,497 kW	224,497 kW	N/A	183,127 kW	11, 439 kW	33,875 kW
Electrolyzer	N/A	1,965 kg/h	3,888 kg/h	1,908 kg/h	2,157 kg/h	2,214 kg/h
Total system cost	$1,112,071,117	$1,033,978,268	$822,851,256	$1,193,795,109	$633,249,296	$767,428,831
Wind curtailment rate	79.1%	21%	0.02%	13.1%	27.4%	21%
LCOH	N/A	$4.07	$5.01	$4.38	$4.52	$4.56

compared to Case I, the batteries in Case II occupy a larger share of the output, leading to an increase in their utilization rate. In Case III, the hydrogen fuel cell fully replaces the function of the conventional battery pack. The results show that the hydrogen fuel cell in Case III effectively substitutes the conventional battery pack and is capable of delivering higher stabilized power output. Comparing Case IV with Case I, the combination of the fuel cell and the battery further optimizes the IES's potential, resulting in higher stabilized power output. Nevertheless, the installed capacity of both the fuel cell and the battery is reduced compared to the previous cases.

These findings underscore the system's adaptability and the strategic allocation of components to achieve higher power output and efficiency. The integration of the hydrogen fuel cell and battery in Case IV demonstrates the potential for improved performance while optimizing component sizes to achieve a balance between system capabilities and resource utilization. The detailed monthly energy output distribution offers valuable insights into the system's performance under varying conditions throughout the year. It highlights how different configurations impact the overall energy distribution among components, providing a clearer understanding of the IES's operation and potential energy savings.

To strike a balance between generality and specificity, the analysis encompasses the system's overall behavior while also zooming in on its specific operational state. Fig. 6 provides insights into the wind power allocation and the state of charging (SOC) of battery and hydrogen tanks within the IES over a randomly selected 168 consecutive hour period for the four cases. This view offers a more detailed perspective on the operational behavior of system components. Notably, the SOC of the battery in Case II exhibits more frequent fluctuations, which is consistent with the observations in Fig. 5. This highlights the dynamic nature of the energy storage system in Case II, where the battery's charge and discharge cycles respond to the variable wind power generation and hydrogen production.

Examining the curtailed rate, the figure reveals that Cases II and III effectively utilize substantial portions of wind energy that would have been curtailed, directing it to the electrolyzer for hydrogen production. This observation aligns with the lower curtailed rates reported in Table 2 for these cases compared to Case I. Furthermore, when comparing wind energy allocation to the electrolyzer in Cases II and IV, it is evident that more curtailed wind energy is efficiently utilized by the electrolyzer in Case IV, in line with the earlier mentioned higher utilization efficiency of the electrolyzer in that case.

Additionally, the SOC of energy storage devices in all four cases during the Hours 40-80 time period, characterized by a relative shortage of wind energy resources, indicates that both batteries and hydrogen tanks play crucial roles in compensating for the IES power output gap during such wind energy shortages. This comprehensive analysis of operational details sheds light on the dynamic behavior and synergistic functioning of system components within the IES.

3.2 Sensitivity Analysis

In Case IV (Comprehensive Integration), three sets of sensitivity analyses were conducted on the IES to assess the impacts of various factors. Firstly, we explored the influence of hydrogen prices on system configurations and parameters. This analysis provided valuable insights into key metrics such as LCOH, total system cost, size of the electrolyzer, and curtailed wind energy rates. Secondly, we examined how different regional wind resources affected the IES. Lastly, we assessed

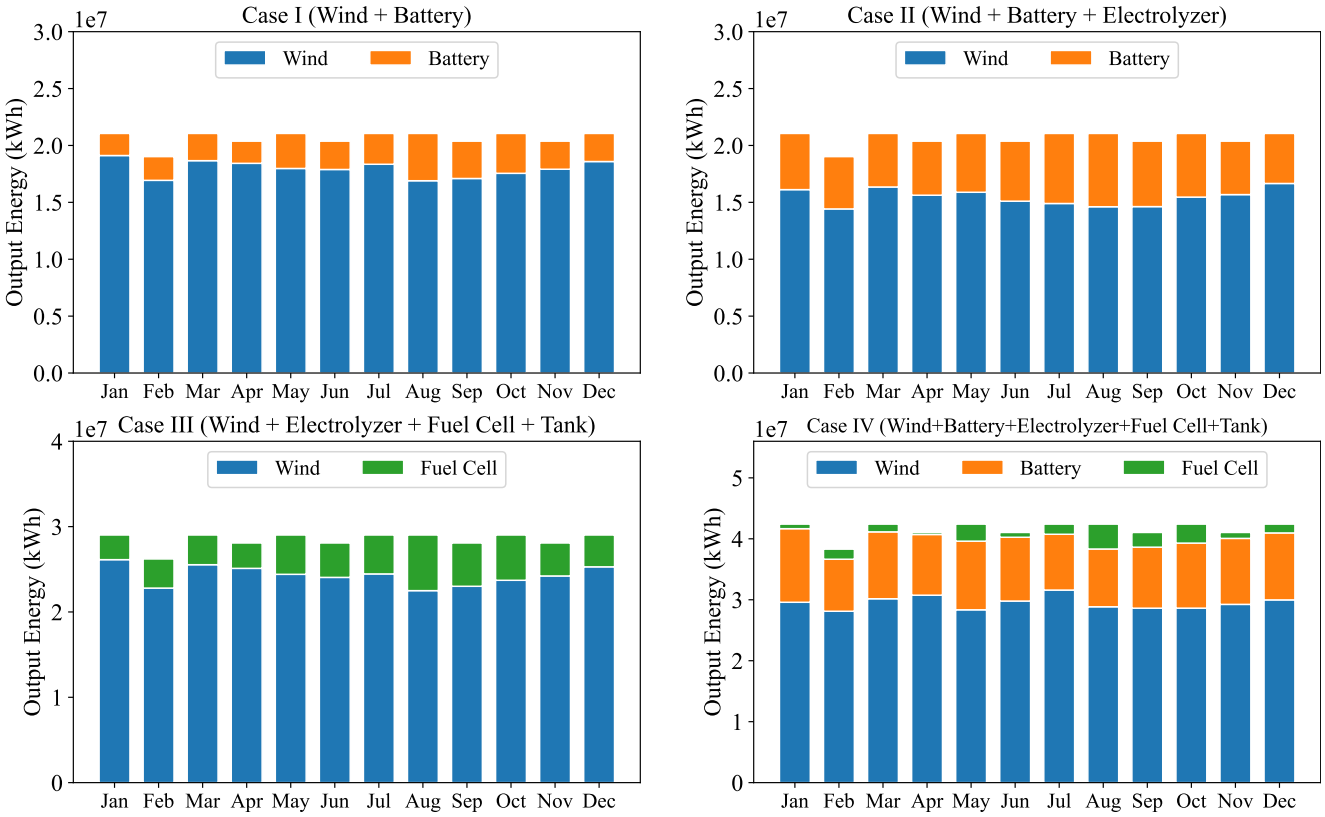


Fig. 5: Monthly output energy of the IES for each component in the four cases

the effects of future component prices on the IES, simulating different price scenarios for wind, battery, electrolyzer, fuel cell, and hydrogen tank installation costs. These analyses offered essential information for decision-making, risk mitigation, and optimized investment strategies, fostering sustainable planning and shaping policies for a resilient and environmentally friendly energy future within the IES.

3.2.1 Impact of Hydrogen Prices on System Configurations

Regarding the impact of hydrogen selling price on the IES, our investigation focused on four key parameters: LCOH, Capital Expenditure (CAPEX) of the IES, size of the electrolyzer in the IES, and the curtailed rate of wind energy within the system. In the baseline Case IV, the selling price of hydrogen was fixed at $2/kg. However, for the sensitivity analysis, we introduced variations in the hydrogen sale price, ranging from $2/kg to $5.5/kg. This allowed us to explore the effects of different price levels, resulting in a total of 8 new simulated cases to assess the influence of these changes.

Fig. 7 illustrates a comprehensible result that emerged from this analysis: as the price of hydrogen increases, the total cost of the IES decreases. This outcome is understandable because the higher hydrogen price leads to increased IES hydrogen revenues, partially offsetting the total system cost. It is also relatively intuitive to observe how the size of the electrolyzer and the curtailed rate of wind energy are affected by the higher hydrogen price. As the hydrogen price rises, the IES tends to install larger electrolyzers to produce more hydrogen, aiming to reduce the total system cost and, consequently, decreasing the amount of wind energy curtailed.

However, one important finding is that the increase in LCOH is mainly due to the larger size of the electrolyzer, which results from the higher hydrogen price. As the size of the electrolyzer increases, the utilization rate of the electrolyzer gradually decreases, leading to a decrease in the hydrogen produced per unit of installed capacity. Consequently, this increase in the LCOH metric is observed. These insights are valuable for understanding the trade-offs and interconnections between hydrogen selling price, system cost, electrolyzer size, and curtailed wind energy within the IES. It informs decision-makers on how to strike a balance between these parameters to achieve cost-effective and efficient operation while ensuring a sustainable and economically viable integrated energy system.

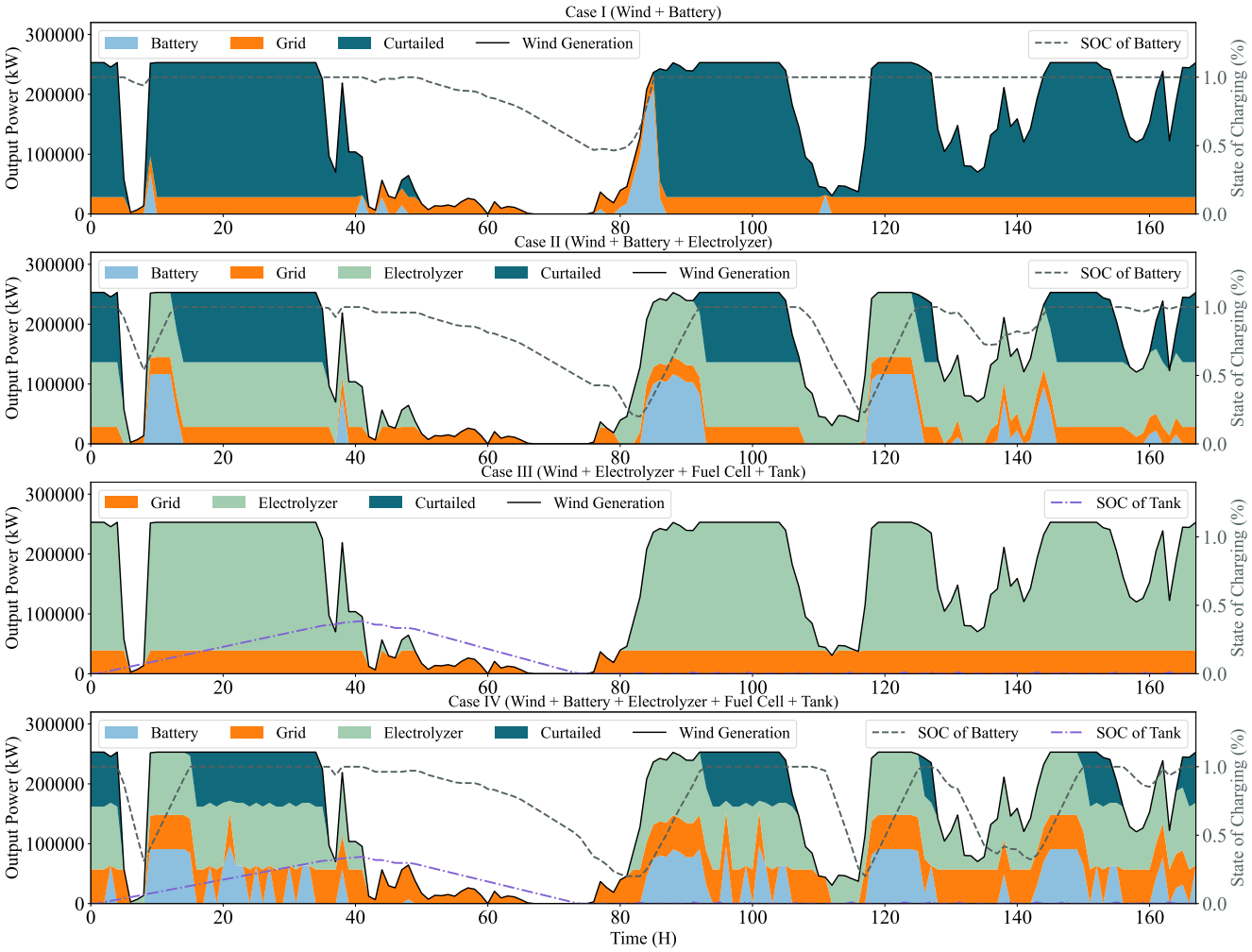


Fig. 6: Hourly wind power allocation and SOC of battery and hydrogen tank within the IES over a randomly selected 168 consecutive hour period. Battery, Grid, and Electrolyzer in the legend represent the hourly wind power allocatioin to the battery, grid, and electrolyzer, respectively. Curtailed and Wind Generation represent wind energy curtailment and actual wind power generation, respectively.

3.2.2 Impact of Regional Variations on System Configurations

To capture regional variations, we consider four distinct wind farms located in strategic regions: the Electric Reliability Council of Texas (ERCOT), the Midcontinent Independent System Operator (MISO), the Southwest Power Pool (SPP), and the Pennsylvania-New Jersey-Maryland Interconnection (PJM). These locations were chosen to represent diverse Independent System Operators (ISOs) with unique wind resource characteristics. For a comprehensive representation, we have provided the geographic coordinates of these locations in Table 3. In this particular sensitivity analysis, we investigate how different wind profiles from diverse regions impact the IES. By thoroughly examining key performance metrics, such as LCOE, LCOH, CAPEX, and curtailed rates under various wind scenarios, this study reveals crucial insights into the system's overall performance and economic viability.

Table 3: The location of the four distinct wind farms located in different ISO regions

	ERCOT	MISO	SPP	PJM
Lon.	-100	-93	-94	-87
Lat.	32	46	40	40

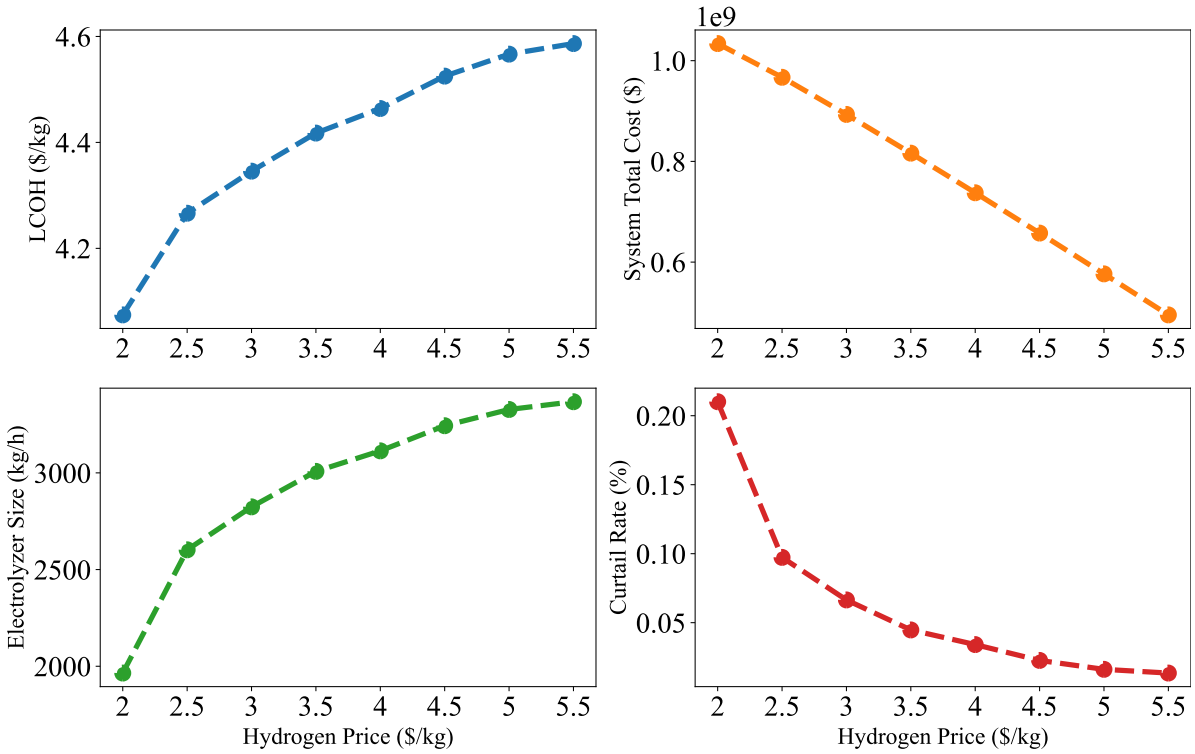


Fig. 7: Sensitivity analysis of the impact of hydrogen price on LCOH, CAPEX, curtail rate price

The outcomes of this sensitivity analysis are depicted in Fig. 8, which showcases how the different wind profiles in each region affect the IES metrics. Among the four wind farms, the one situated in ERCOT stands out with the most abundant wind resource, resulting in the lowest LCOE, LCOH, and CAPEX, while concurrently exhibiting the highest curtailed rate. This valuable information aids in understanding the strengths and challenges associated with each region's wind resources, guiding strategic decision-making and potential investment opportunities for achieving enhanced system performance and cost-effectiveness within the IES.

The ERCOT wind farm's favorable outcomes highlight its potential as an attractive location for renewable energy integration and hydrogen-based storage. The abundance of wind resources leads to lower LCOE and LCOH, making the electricity and hydrogen produced in this region more competitive in the energy market. Additionally, the reduced CAPEX indicates that the initial investment required for establishing the IES is relatively lower in ERCOT, potentially attracting investors and stakeholders interested in sustainable energy projects. However, the high curtailed rate observed in ERCOT suggests a challenge in efficiently utilizing the surplus wind energy. This finding calls for innovative energy storage strategies, such as hydrogen production and storage, to effectively capture and store excess energy during periods of high wind generation.

Conversely, wind farms in other regions, such as MISO, SPP, and PJM, exhibit different trade-offs. While these regions may have higher LCOE, LCOH, and CAPEX due to relatively lower wind resources, they also experience reduced curtailed rates, indicating better utilization of wind energy. These regions may have a higher focus on optimizing energy storage solutions and balancing mechanisms to align electricity supply with demand. To offer decision makers a more comprehensive grasp of the interrelationships among the four systematic evaluation metrics, we have further summarized their connections as follows. **LCOE and Wind Resource:** Our analysis reveals that LCOE remains consistent across all cases, signifying its primary association with the wind resource available at a specific location. Areas with superior wind resources tend to exhibit lower LCOE, and vice versa. **LCOH and LCOE Correlation:** There exists a positive correlation between LCOH and LCOE due to the significant influence of electricity, a major cost component in hydrogen production, shared by both metrics. **CAPEX and Cost Metrics:** CAPEX is found to be lower when both LCOE and LCOH exhibit lower values, although the correlation is not extremely strong. This suggests that reducing operational costs can potentially lead to reduced capital costs. **Curtailment Rate:** The curtailment rate is influenced by various factors such as wind resource volatility and system configuration. It is suggested that considering wind curtailment rate as an additional optimization objective in future research could facilitate multi-objective optimization and provide deeper insights.

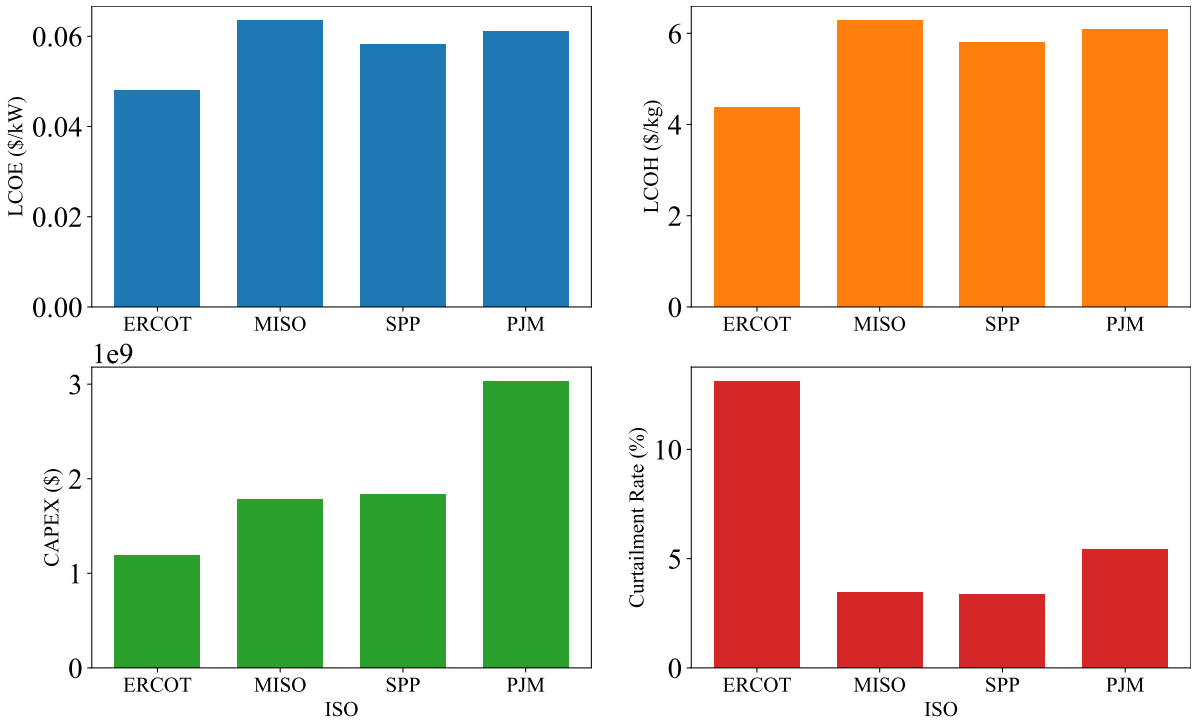


Fig. 8: Sensitivity analysis of the impact of wind profile in different regions on LCOE, LCOH, CAPEX, and curtailed rate

Table 4: Annual Technology Baseline ($/kW) [46–49]

Year	CAPEX					O&M				
	Wind	Battery [a]	Electrolyzer	Fuel Cell	Tank	Wind	Battery [b]	Electrolyzer	Fuel Cell	Tank [c]
2020	1,874	840	48,000	500	1,168	40	410	3,600	30	116.8
2025	1,323	838	46,000	450	1,110	35	400	3,500	28	111
2030	1,274	620	44,000	400	1,070	34	340	3,400	26	107
2035	1,231	512	42,000	350	1,040	33	328	3,300	25	104
2040	1,188	454	40,000	300	1,010	32	313	3,200	24	101
2045	1,145	410	38,000	250	980	31	300	3,100	23	98
2050	1,102	346	36,000	200	950	30	289	3,000	22	95

[a] Battery CAPEX: Total upfront battery power capacity costs; energy capacity cost is half of it.
[b] Battery O&M: Battery power capacity replacement cost at time of replacement year.
[c] Tank Cost Unit: $/kg.

3.2.3 Impact of Future Component Prices on System Configurations

The final set of sensitivity analyses investigates the influence of component prices within the IES on key performance metrics over a thirty-year horizon [46–49], as presented in Table 4. As technology matures, the prices of these components are expected to decline. This analysis aims to assess how fluctuations in prices for components like wind, battery, electrolyzer, fuel cell, and hydrogen tank installation costs impact critical IES metrics, including LCOE, LCOH, CAPEX, wind curtailed rate, and system component sizes.

By understanding the implications of future component prices on the IES, stakeholders can make informed decisions, mitigate risks, and devise optimized investment strategies. It facilitates sustainable planning, policy formation, and ensures long-term sustainability. Moreover, this analysis offers competitive advantages, fosters public acceptance, and aids in resource allocation. The comprehension of how price fluctuations influence key IES metrics enables the development of

cost-effective, resilient, and environmentally friendly energy solutions for a sustainable future.

Fig. 9 illustrates the temporal evolution of each key IES metric and component sizes as prices decrease. Financial metrics, such as LCOE, LCOH, and CAPEX, exhibit a progressive reduction. As component prices decrease, the overall cost of electricity and hydrogen production decreases, leading to more economically viable solutions. Additionally, the electrolyzer size increases with decreasing prices, enabling better utilization of curtailed wind energy and consequently lowering the wind curtailed rate. The larger electrolyzer capacity allows for more efficient conversion of excess wind energy into hydrogen, maximizing the system's energy utilization. However, the sizes of storage devices and hydrogen fuel cells remain unchanged, primarily due to their limited sensitivity to price variations as essential support components for IES operations.

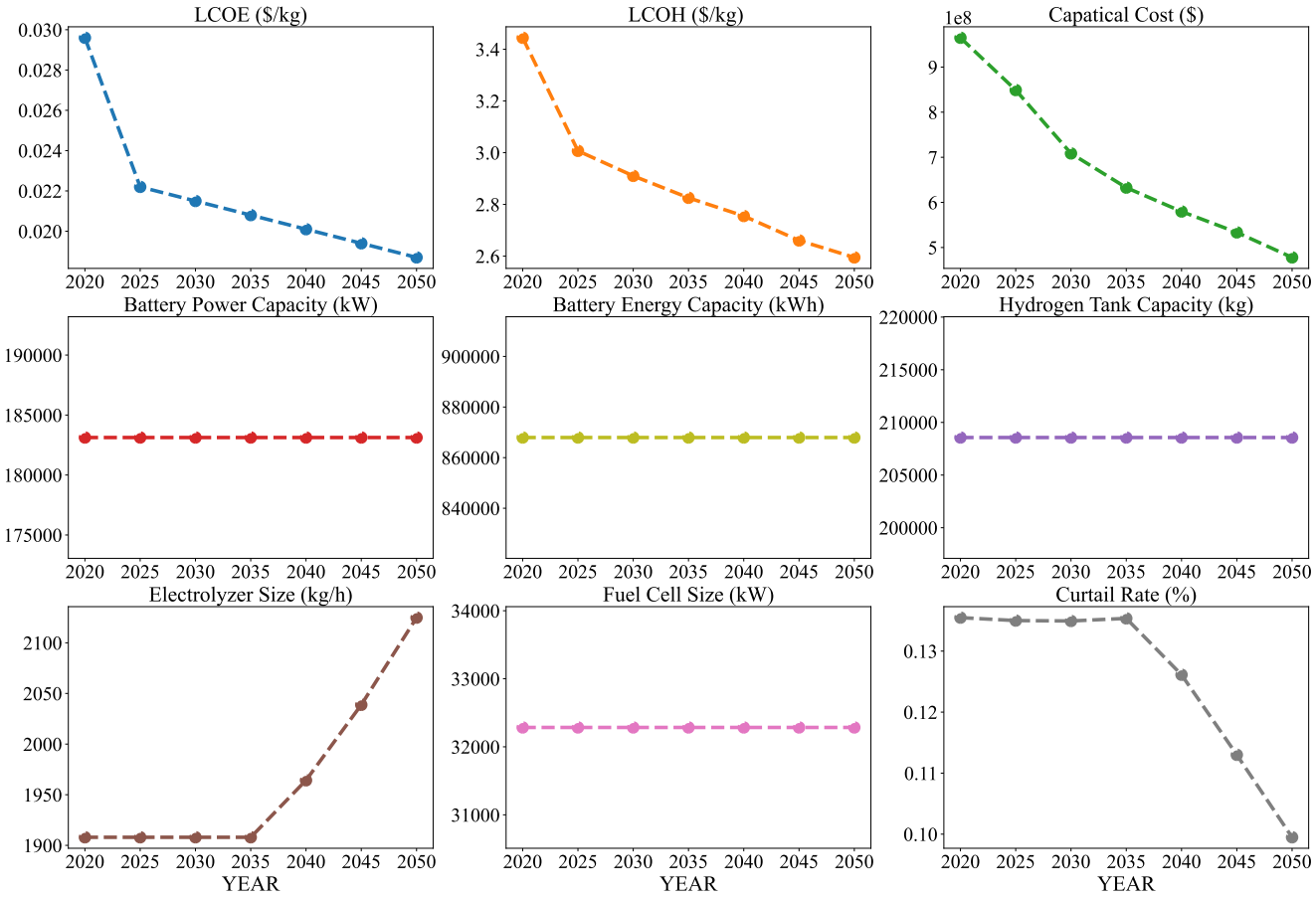


Fig. 9: Sensitivity analysis of future components' prices

4 Conclusion

In this research, we conducted a comprehensive techno-economic analysis of co-located wind and hydrogen energy within an Integrated Energy System (IES) to explore cost-effective and sustainable energy solutions. It was found that comparing to configurations that only have wind and conventional battery combinations, incorporating an electrolyzer results in a 7% reduction in the total cost of the IES, and utilizing hydrogen as the energy storage medium for hydrogen fuel cells leads to a 26% cost reduction.

The sensitivity analysis of hydrogen prices revealed that higher hydrogen selling prices led to reduced total system costs due to increased hydrogen revenues, thus partially offsetting IES expenses. Moreover, as the hydrogen price increased, the IES strategically installed larger electrolyzers to convert excess wind energy into hydrogen, resulting in a significant reduction of wind curtailment rates.

Investigating regional wind profiles allowed us to identify ERCOT as a region with the most abundant wind resource, resulting in the lowest LCOE. However, the high curtailed rate in ERCOT indicated the need for further consideration of grid limitations and operational challenges in the region.

The analysis of future component prices illustrated a progressive reduction in financial metrics, such as LCOE, LCOH, and CAPEX, with decreasing costs over the thirty-year horizon. The increase in the size of the electrolyzer with decreasing prices led to improved utilization of excess wind energy and a decrease in wind curtailment rates. This demonstrates the system's adaptability to changing technology costs and its potential for enhanced cost-effectiveness over time.

Overall, our research offers valuable insights for decision-makers and planners seeking to develop sustainable, resilient, and environmentally friendly energy solutions within an IES. By considering diverse scenarios and specific data findings, stakeholders can strategically allocate resources, optimize component selections, and devise investment strategies that align with long-term objectives and market dynamics. This holistic approach to techno-economic analysis empowers stakeholders to make informed decisions, mitigate risks, and shape policies that foster a sustainable and economically viable energy future. By harnessing the potential of co-located wind and hydrogen energy, we pave the way for a greener and more sustainable energy landscape, contributing to a resilient and carbon-neutral future.

Future research directions in the field of co-located wind and hydrogen energy within IES hold significant potential for advancing sustainable energy solutions. Continued investigation into the optimization of component configurations and sizing strategies can further enhance system performance and economic feasibility. Additionally, exploring advanced energy storage technologies, such as advanced batteries and novel hydrogen storage solutions, can improve the overall efficiency and reliability of the IES. Integration of advanced forecasting and control algorithms can also be explored to better manage the variability of renewable energy sources and enhance grid stability. Furthermore, research on the scalability and replicability of IES models in different geographic regions will be valuable for widespread implementation and adoption. Lastly, considering the social and environmental impacts of IES deployment can contribute to fostering community acceptance and promoting sustainable development in the energy sector.

Acknowledgements

This material is based upon work supported by the National Science Foundation under Grant Number 1916776 (Phase II IUCRC at UT Dallas: Center for Wind Energy Science, Technology and Research (WindSTAR)) and the WindSTAR I/UCRC Members. Any opinions, findings, and conclusions or recommendations expressed in this material are those of the author(s) and do not necessarily reflect the views of the National Science Foundation or WindSTAR members.

References

[1] Li, H., Kiviluoma, J., and Zhang, J., 2023. "Techno-economic analysis for co-located solar and hydrogen plants". In 2023 19th International Conference on the European Energy Market (EEM), IEEE, pp. 1–6.

[2] Agreement, P., 2015. "Paris agreement". In report of the conference of the parties to the United Nations framework convention on climate change (21st session, 2015: Paris). Retrived December, Vol. 4, HeinOnline, p. 2017.

[3] Herbert, G. J., Iniyan, S., Sreevalsan, E., and Rajapandian, S., 2007. "A review of wind energy technologies". *Renewable and sustainable energy Reviews,* **11**(6), pp. 1117–1145.

[4] IEA. Wind. [Online] Available at: `https://www.iea.org/energy-system/renewables/wind`. [Accessed: 24 Jul. 2023].

[5] Lin, H., Wu, Q., Chen, X., Yang, X., Guo, X., Lv, J., Lu, T., Song, S., and McElroy, M., 2021. "Economic and technological feasibility of using power-to-hydrogen technology under higher wind penetration in china". *Renewable Energy,* **173**, pp. 569–580.

[6] Badakhshan, S., Senemmar, S., Li, H., and Zhang, J., 2022. "Integrating offshore wind farms with unmanned hydrogen and battery ships". In 2022 IEEE Kansas Power and Energy Conference (KPEC), IEEE, pp. 1–6.

[7] Feng, C., Cui, M., Hodge, B.-M., and Zhang, J., 2017. "A data-driven multi-model methodology with deep feature selection for short-term wind forecasting". *Applied Energy,* **190**, pp. 1245–1257.

[8] Sun, M., Feng, C., Chartan, E. K., Hodge, B.-M., and Zhang, J., 2019. "A two-step short-term probabilistic wind forecasting methodology based on predictive distribution optimization". *Applied energy,* **238**, pp. 1497–1505.

[9] Barra, P., De Carvalho, W., Menezes, T., Fernandes, R., and Coury, D., 2021. "A review on wind power smoothing using high-power energy storage systems". *Renewable and Sustainable Energy Reviews,* **137**, p. 110455.

[10] Howlader, A. M., Urasaki, N., Yona, A., Senjyu, T., and Saber, A. Y., 2013. "A review of output power smoothing methods for wind energy conversion systems". *Renewable and Sustainable Energy Reviews,* **26**, pp. 135–146.

[11] Qais, M. H., Hasanien, H. M., and Alghuwainem, S., 2020. "Output power smoothing of wind power plants using self-tuned controlled smes units". *Electric power systems research,* **178**, p. 106056.

[12] Khalid, M., and Savkin, A. V., 2010. "A model predictive control approach to the problem of wind power smoothing with controlled battery storage". *Renewable Energy,* **35**(7), pp. 1520–1526.

[13] Diaz-Gonzalez, F., Bianchi, F. D., Sumper, A., and Gomis-Bellmunt, O., 2013. "Control of a flywheel energy storage system for power smoothing in wind power plants". *IEEE Transactions on Energy Conversion,* **29**(1), pp. 204–214.

[14] Li, X., Hui, D., and Lai, X., 2013. "Battery energy storage station (bess)-based smoothing control of photovoltaic (pv) and wind power generation fluctuations". *IEEE transactions on sustainable energy,* **4**(2), pp. 464–473.

[15] Dinglin, L., Yingjie, C., Kun, Z., and Ming, Z., 2012. "Economic evaluation of wind-powered pumped storage system". *Systems Engineering Procedia,* **4**, pp. 107–115.

[16] Hasan, N., Hassan, M., Majid, M., and Rahman, H., 2012. "Mathematical model of compressed air energy storage in smoothing 2mw wind turbine". In 2012 IEEE International Power Engineering and Optimization Conference Melaka, Malaysia, IEEE, pp. 339–343.

[17] Shaqsi, A. Z. A., Sopian, K., and Al-Hinai, A., 2020. "Review of energy storage services, applications, limitations, and benefits". *Energy Reports,* **6**, pp. 288–306.

[18] Rahman, J., Jacob, R. A., and Zhang, J., 2022. "Harnessing operational flexibility from power to hydrogen in a grid-tied integrated energy system". In International Design Engineering Technical Conferences and Computers and Information in Engineering Conference, Vol. 86229, American Society of Mechanical Engineers, p. V03AT03A022.

[19] Wang, Z., Zhang, X., and Rezazadeh, A., 2021. "Hydrogen fuel and electricity generation from a new hybrid energy system based on wind and solar energies and alkaline fuel cell". *Energy Reports,* **7**, pp. 2594–2604.

[20] Herwartz, S., Pagenkopf, J., and Streuling, C., 2021. "Sector coupling potential of wind-based hydrogen production and fuel cell train operation in regional rail transport in berlin and brandenburg". *International Journal of Hydrogen Energy,* **46**(57), pp. 29597–29615.

[21] Kudria, S., Ivanchenko, I., Tuchynskyi, B., Petrenko, K., Karmazin, O., and Riepkin, O., 2021. "Resource potential for wind-hydrogen power in ukraine". *International Journal of Hydrogen Energy,* **46**(1), pp. 157–168.

[22] Li, N., Zhao, X., Shi, X., Pei, Z., Mu, H., and Taghizadeh-Hesary, F., 2021. "Integrated energy systems with cchp and hydrogen supply: A new outlet for curtailed wind power". *Applied Energy,* **303**, p. 117619.

[23] Kakoulaki, G., Kougias, I., Taylor, N., Dolci, F., Moya, J., and Jäger-Waldau, A., 2021. "Green hydrogen in europe–a regional assessment: Substituting existing production with electrolysis powered by renewables". *Energy Conversion and Management,* **228**, p. 113649.

[24] Ayodele, T., and Munda, J., 2019. "Potential and economic viability of green hydrogen production by water electrolysis using wind energy resources in south africa". *International Journal of Hydrogen Energy,* **44**(33), pp. 17669–17687.

[25] Iqbal, W., Yumei, H., Abbas, Q., Hafeez, M., Mohsin, M., Fatima, A., Jamali, M. A., Jamali, M., Siyal, A., and Sohail, N., 2019. "Assessment of wind energy potential for the production of renewable hydrogen in sindh province of pakistan". *Processes,* **7**(4), p. 196.

[26] Rahman, J., Jacob, R., and Zhang, J., 2023. "Multi-timescale power system operations for electrolytic hydrogen generation in integrated nuclear-renewable energy systems".

[27] Buffi, M., Prussi, M., and Scarlat, N., 2022. "Energy and environmental assessment of hydrogen from biomass sources: Challenges and perspectives". *Biomass and Bioenergy,* **165**, p. 106556.

[28] Ogbonnaya, C., Abeykoon, C., Nasser, A., and Turan, A., 2021. "Unitized regenerative proton exchange membrane fuel cell system for renewable power and hydrogen generation: Modelling, simulation, and a case study". *Cleaner Engineering and Technology,* **4**, p. 100241.

[29] Shen, Y., Li, X., Wang, N., Li, L., and Hoseyni, A., 2021. "Introducing and investigation of a pumped hydro-compressed air storage based on wind turbine and alkaline fuel cell and electrolyzer". *Sustainable Energy Technologies and Assessments,* **47**, p. 101378.

[30] da Silva, G. N., Rochedo, P. R., and Szklo, A., 2022. "Renewable hydrogen production to deal with wind power surpluses and mitigate carbon dioxide emissions from oil refineries". *Applied Energy,* **311**, p. 118631.

[31] Elberry, A. M., Thakur, J., Santasalo-Aarnio, A., and Larmi, M., 2021. "Large-scale compressed hydrogen storage as part of renewable electricity storage systems". *International journal of hydrogen energy,* **46**(29), pp. 15671–15690.

[32] Hassanpouryouzband, A., Joonaki, E., Edlmann, K., and Haszeldine, R. S., 2021. "Offshore geological storage of hydrogen: is this our best option to achieve net-zero?". *ACS Energy Letters,* **6**(6), pp. 2181–2186.

[33] Liu, B., Liu, S., Guo, S., and Zhang, S., 2020. "Economic study of a large-scale renewable hydrogen application utilizing surplus renewable energy and natural gas pipeline transportation in china". *International Journal of Hydrogen Energy,* **45**(3), pp. 1385–1398.

[34] He, W., Zheng, Y., You, S., Strbac, G., Therkildsen, K. T., Olsen, G. P., Howie, A., Byklum, E., and Sharifabadi, K. T., 2022. "Case study on the benefits and risks of green hydrogen production co-location at offshore wind farms". In Journal of Physics: Conference Series, Vol. 2265, IOP Publishing, p. 042035.

[35] Farag, H. E., Al-Obaidi, A., Khani, H., El-Taweel, N., El-Saadany, E., and Zeineldin, H., 2020. "Optimal operation management of distributed and centralized electrolysis-based hydrogen generation and storage systems". *Electric Power Systems Research,* **187**, p. 106476.

[36] Li, H., Rahman, J., and Zhang, J., 2022. "Optimal planning of co-located wind energy and hydrogen plants: A techno-economic analysis". In Journal of Physics: Conference Series, Vol. 2265, IOP Publishing, p. 042063.

[37] Rezaei, M., Khalilpour, K. R., and Mohamed, M. A., 2021. "Co-production of electricity and hydrogen from wind: A comprehensive scenario-based techno-economic analysis". *International Journal of Hydrogen Energy,* **46**(35),

pp. 18242–18256.
[38] Giampieri, A., Ling-Chin, J., and Roskilly, A. P., 2023. "Techno-economic assessment of offshore wind-to-hydrogen scenarios: A uk case study". *International Journal of Hydrogen Energy*.
[39] Dabar, O. A., Awaleh, M. O., Waberi, M. M., and Adan, A.-B. I., 2022. "Wind resource assessment and techno-economic analysis of wind energy and green hydrogen production in the republic of djibouti". *Energy reports,* **8**, pp. 8996–9016.
[40] Kong, L., Li, L., Cai, G., Liu, C., Ma, P., Bian, Y., and Ma, T., 2021. "Techno-economic analysis of hydrogen energy for renewable energy power smoothing". *International Journal of Hydrogen Energy,* **46**(3), pp. 2847–2861.
[41] Mishra, S., Pohl, J., Laws, N., Cutler, D., Kwasnik, T., Becker, W., Zolan, A., Anderson, K., Olis, D., and Elgqvist, E., 2022. "Computational framework for behind-the-meter der techno-economic modeling and optimization: Reopt lite". *Energy Systems,* **13**(2), pp. 509–537.
[42] Saur, G., 2008. Wind-to-hydrogen project: electrolyzer capital cost study. Tech. rep., National Renewable Energy Lab.(NREL), Golden, CO (United States).
[43] Connelly, E., Penev, M., Milbrandt, A., Roberts, B., Melaina, M. W., and Gilroy, N., 2020. "Resource assessment for hydrogen production".
[44] Ruth, M. F., Jadun, P., Gilroy, N., Connelly, E., Boardman, R., Simon, A., Elgowainy, A., and Zuboy, J., 2020. The technical and economic potential of the h2@ scale hydrogen concept within the united states. Tech. rep., National Renewable Energy Lab.(NREL), Golden, CO (United States).
[45] Parks, G., Boyd, R., Cornish, J., and Remick, R., 2014. Hydrogen station compression, storage, and dispensing technical status and costs: Systems integration. Tech. rep., National Renewable Energy Lab.(NREL), Golden, CO (United States).
[46] NREL. Annual technology baseline. [Online] Available at: `https://atb.nrel.gov/`. [Accessed: 25 Jul. 2023].
[47] Schmidt, O., Gambhir, A., Staffell, I., Hawkes, A., Nelson, J., and Few, S., 2017. "Future cost and performance of water electrolysis: An expert elicitation study". *International journal of hydrogen energy,* **42**(52), pp. 30470–30492.
[48] Offer, G. J., Howey, D., Contestabile, M., Clague, R., and Brandon, N., 2010. "Comparative analysis of battery electric, hydrogen fuel cell and hybrid vehicles in a future sustainable road transport system". *Energy policy,* **38**(1), pp. 24–29.
[49] Alirahmi, S. M., Razmi, A. R., and Arabkoohsar, A., 2021. "Comprehensive assessment and multi-objective optimization of a green concept based on a combination of hydrogen and compressed air energy storage (caes) systems". *Renewable and Sustainable Energy Reviews,* **142**, p. 110850.